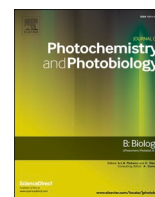




Contents lists available at ScienceDirect

Journal of Photochemistry & Photobiology, B: Biology

journal homepage: www.elsevier.com/locate/jphotobiol

Molecular characteristics of the photosensitizer TONS504: Comparison of its singlet oxygen quantum yields and photodynamic antimicrobial effect with those of methylene blue

Koichiro Shinji^a, Taiichiro Chikama^{a,*}, Shigetoshi Okazaki^b, Yoshihiro Uto^c, Kentaro Sueoka^a, Yuniathy Dwia Pertiwi^d, Ji-Ae Ko^a, Yoshiaki Kiuchi^a, Takemasa Sakaguchi^e

^a Department of Ophthalmology and Visual Science Graduate School of Biomedical Sciences, Hiroshima University, Hiroshima 734-8551, Japan

^b HAMAMATSU BioPhotonics Innovation Chair, Preeminent Medical Photonics Education & Research Center, Hamamatsu University School of Medicine, Hamamatsu, Shizuoka 431-3192, Japan

^c Graduate School of Technology, Industrial and Social Science, Tokushima University, Tokushima 770-8506, Japan

^d Department of Microbiology, Faculty of Medicine, Hasanuddin University, Makassar, South Sulawesi 90245, Indonesia

^e Department of Virology, Graduate School of Biomedical Sciences, Hiroshima University, Hiroshima, 734-8551, Japan

ARTICLE INFO

Keywords:

Photochemotherapy
Antimicrobial resistance
TONS504
Methylene blue
Singlet oxygen

ABSTRACT

TONS504 (C51H58O5I2) is a chlorin derivative that exhibits a photodynamic antimicrobial effect (PAE) on various infectious keratitis pathogens. However, the molecular characteristics of TONS504 are not well understood. This study aimed to investigate the molecular characteristics of TONS504 by comparing its singlet oxygen ($^1\text{O}_2$) quantum yields and PAE with those of methylene blue (MB). To measure the $^1\text{O}_2$ quantum yields, TONS504 and MB were dissolved in phosphate-buffered saline and phosphate-buffered saline containing 1% Triton X-100. The solutions were then activated by a Nd:YAG laser with an average output power of 8 mW. Near-infrared $^1\text{O}_2$ luminescence was detected as an indicator of the $^1\text{O}_2$ quantum yields. To evaluate the PAE, TONS504 and MB were activated by a light-emitting diode with a total light energy of 30 J/cm². We compared the minimum molar concentration of each photosensitizer to show apparent PAEs on *Staphylococcus aureus*, *Pseudomonas aeruginosa*, and *Candida albicans*. TONS504 exhibited higher $^1\text{O}_2$ quantum yields than MB in PBS/Triton X-100 but not in PBS. *S. aureus* and *C. albicans* were reduced by TONS504 at lower concentrations than by MB, but this was not the case for *P. aeruginosa*. Our results provide insight on the molecular characteristics of TONS504 and suggest that TONS504 has excellent $^1\text{O}_2$ quantum yields and PAE. Compared with MB, TONS504 in PBS has stronger efficacy toward some infectious keratitis pathogens but not others.

1. Introduction

Infectious keratitis results in corneal opacity and eventually vision loss if it is not managed appropriately. According to a systematic review, non-trachomatous corneal opacities are ranked as the fifth leading cause of vision loss [1]. Antibiotic agents are currently the most reliable and widely accepted treatment for infectious keratitis. However, the overuse of broad-spectrum antibiotics without an appropriate diagnosis accelerates increases in antimicrobial resistance in both bacterial and fungal

keratitis [2–4]. Therefore, alternative approaches for combating infectious keratitis are urgently required.

Photodynamic antimicrobial chemotherapy (PACT), which is also known as antimicrobial photodynamic therapy or photodynamic antimicrobial therapy, is one of the promising non-antibiotic strategies to manage infectious diseases [5]. PACT involves the synergistic action of three components: a photosensitizer, light with a specific wavelength to activate the photosensitizer, and molecular oxygen [6]. This interaction generates reactive oxygen species, such as singlet oxygen ($^1\text{O}_2$), which

Abbreviations: PAE, photodynamic antimicrobial effect; MB, methylene blue; PACT, photodynamic antimicrobial chemotherapy; CXL, corneal cross-linking.

* Corresponding author at: Department of Ophthalmology and Visual Science, Graduate School of Biomedical and Health Sciences, Hiroshima University, 1-2-3 Kasumi, Minami-ku, Hiroshima 734-8551, Japan.

E-mail addresses: shinjiko@hiroshima-u.ac.jp (K. Shinji), chikama@hiroshima-u.ac.jp (T. Chikama), okazaki@hama-med.ac.jp (S. Okazaki), uto.yoshihiro@tokushima-u.ac.jp (Y. Uto), ksueoka@hiroshima-u.ac.jp (K. Sueoka), jiaeko@hiroshima-u.ac.jp (J.-A. Ko), ykiuchi@hiroshima-u.ac.jp (Y. Kiuchi), tsaka@hiroshima-u.ac.jp (T. Sakaguchi).

<https://doi.org/10.1016/j.jphotobiol.2021.112239>

Received 27 March 2021; Received in revised form 24 May 2021; Accepted 2 June 2021

1011-1344/© 2021 Elsevier B.V. All rights reserved.

destroy various molecular targets [7]. PACT exhibits an antimicrobial effect toward multiple pathogens, including antimicrobial resistant strains, and is unlikely to induce resistance because of its non-selective approach with various targets [8].

Initial PACT approaches for the management of infectious keratitis have used riboflavin and ultraviolet A light for corneal cross-linking (CXL) [9–11]. Corneal cross-linking has been applied as an adjunctive therapy of infectious keratitis with limited efficacy [12]. According to several, rose bengal, which is widely used as a diagnostic dye in ophthalmology [13], exhibits a stronger a photodynamic antimicrobial effect (PAE) than riboflavin [14–16]. This research shows that PACT is a promising post-antimicrobial therapy to manage infectious keratitis, and rose bengal is a major candidate for use in this approach. However, rose bengal has a relatively short absorption range (450–650 nm) and anionic charge [17,18] and photosensitizers with absorption maxima at longer wavelengths and cationic charges are thought to be more suitable for PACT [19,20]. Therefore, better photosensitizers should be identified for treatment of infectious keratitis.

We have evaluated the effect of PACT for various infectious keratitis causative microorganisms using a newly developed photosensitizer called TONS504 [13,17-bis(1-carboxyethyl)-carbamoyl-(3-methylpyridine)-3-(1,3-dioxane-2-yl) methylidene-8-ethenyl-2-hydroxy-2,7,12,18-tetramethyl chlorin, di-*N*-methyl iodide (C₅₁H₅₈O₅I₂)], a hydrophilic and cationic chlorin derivative with a greenish color and molecular weight of 1116 Da (Fig. 1) [21–26]. However, its molecular characteristics, such as its ¹O₂ quantum yields, hydrophilicity, and tendency to self-aggregate, are not well understood.

The present study aimed to investigate the molecular characteristics of TONS504 through a comparison with another photosensitizer. To standardize the experimental conditions the other photosensitizer needed to be excited by the same wavelength of light as TONS504 because the wavelength affects the efficacy of photodynamic therapy [27]. Methylene blue (MB) is widely used as a photosensitizer for PACT. It has strong absorption between 630 and 680 nm [28], and this range contains the wavelength for activation of TONS504 in chloroform detected in a prior experiment. We compared the PAEs of TONS504 and MB using their molecular characteristics. The target organisms were *Staphylococcus aureus*, *Pseudomonas aeruginosa*, and *Candida albicans*.

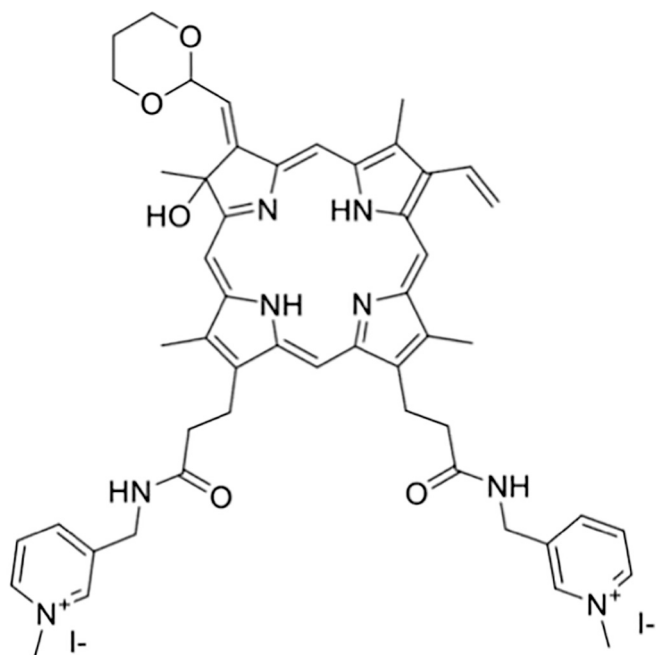


Fig. 1. Chemical structure of TONS504. The chlorin ring has hydrophilic side chains containing one hydroxy group and pyridinium groups.

These microorganisms are important causative pathogens of infectious keratitis and cover the classes of Gram-positive bacteria, Gram-negative bacteria, and fungi [2].

2. Materials and Methods

2.1. Photosensitizers and Light Sources

To evaluate the ¹O₂ quantum yields, separate stock solutions of 1 mmol/L TONS504 (Porphyrin Laboratory, Okayama, Japan) and 2 mmol/L MB (Sigma-Aldrich, St. Louis, MO, USA) dissolved in phosphate-buffered saline (PBS, pH 7.4) were prepared. Each solution was further diluted in PBS or PBS containing 1% Triton X-100 (PBS/TX100, Sigma-Aldrich) to concentrations of 1, 2, or 5 μmol/L (TONS504) and 1 or 2 μmol/L (MB). A pulsed tunable dye laser (CL-EGC, Usho Optical Systems, Osaka, Japan) excited by a Nd:YAG laser (NL204/SH, Ekspla, Vilnius, Lithuania) was used as the light source for measurement of ¹O₂ luminescence. This provided a pulse width of around 5 ns and a repetition frequency of 500 Hz. The laser dye [2-[2-(4-(dimethylamino) phenyl) ethenyl]-6-methyl-4H-pyran-4-ylidene]-propanedinitrile (06490, Exciton, West Chester, OH, USA) was used for excitation at a wavelength of 664 nm. The average output power was set at 8 mW.

For evaluating the PAE, we prepared separate stock solutions (0.9 mmol/L) of TONS504 and MB by dissolving the powdered chemicals in PBS. The TONS504 and MB solutions were further diluted in PBS to evaluate the antimicrobial activity at various concentrations (9.0 × 10⁻³ to 9.0 μmol/L for TONS504, and 9.0 × 10⁻¹ to 900 μmol/L for MB). The light source for PACT was a light-emitting diode system (ME-PT-DSRD660–0201, CCS, Kyoto, Japan) that emitted light centered at a wavelength of 660 nm. The irradiance of the light source was 0.055 W/cm², which was measured with an optical power meter (Hioki, Nagano, Japan). Light irradiation was performed for 9 min continuously to obtain a total light energy of 30 J/cm². TONS504 exhibited higher ¹O₂ quantum yields than MB in PBS/TX100 but not in PBS.

2.2. Measurement of ¹O₂ Luminescence

First, the absorption spectra of the TONS504 and MB solutions in PBS or PBS/TX100 were measured by a spectrophotometer (U-3500, Hitachi, Tokyo, Japan). To assess the ¹O₂ quantum yields, we measured the ¹O₂ luminescence at the near-infrared (NIR) wavelength [29]. The strategy used to measure ¹O₂ luminescence followed that described in previous studies with some modifications [29,30]. Briefly, the NIR luminescence of the sample was collimated by optical lenses and collected into a polychromator (250is, Chromex, Albuquerque, NM, US). The luminescence spectra were detected by an infrared-gated image intensifier (NIR-PII, Hamamatsu Photonics K.K., Shizuoka, Japan) at the exit port of the polychromator. To measure the luminescence decay curve, the NIR luminescence from the samples was also fed to a flexible quartz-fiber bundle and guided to a band-pass filter unit (central wavelength of 1275 nm, and full width at half maximum of 50 nm; H9170FSU, Hamamatsu Photonics K.K.), detected, and converted to a signal by a photomultiplier (H10330–45, Hamamatsu Photonics K.K.). The signal was analyzed by a multichannel scaler (NanoHarp-250, PicoQuant, Berlin, Germany) to obtain the time-resolved ¹O₂ luminescence decay curve over 50 μs. The decay curves were corrected for absorptivity.

2.3. Microorganisms and Culture Conditions

Staphylococcus aureus (NITE Biological Resource Center 14,462) and *P. aeruginosa* (American Type Culture Collection 27,853) were grown in a liquid medium, containing hipolypepton (Nihon Pharmaceutical, Tokyo, Japan), magnesium sulfate heptahydrate, and extract yeast dried (Nacalai Tesque, Kyoto, Japan) at 37 °C overnight in a shaking incubator. *Candida albicans* (NITE Biological Resource Center 1594) was

grown in YM liquid medium containing D-glucose, extract yeast dried, malt extract (Nacalai Tesque), and Mikuni peptone (Mikuni Chemical Industry, Tokyo, Japan), for 48 to 72 h at 24 °C in a shaking incubator. The pellet of each strain was collected by centrifugation at 3000 ×g for 10 min at 4 °C and washed three times with PBS. Each pellet was resuspended in sufficient PBS to adjust the concentration to 1 × 10⁷ colony-forming units (CFU)/mL, which was measured using a spectrophotometer (NanoDrop 2000c, Thermo Fisher Scientific, Waltham, MA, USA).

2.4. PACT and Antibacterial Assays

Ten microliters of each microbial suspension was transferred to a 24-well plate and mixed with 1 mL of TONS504 or MB solution. To evaluate the toxicity of irradiation on its own, the microbial suspensions were also mixed with PBS without any photosensitizers. After incubation for 5 min at room temperature, the 24-well plate was uncovered and placed 5 cm below the light-emitting diode system. The plate was exposed to light for 9 min continuously with a total light energy of 30 J/cm². The toxicities of the photosensitizers in the dark were simultaneously measured for microbial–photosensitizer mixtures without light exposure. Immediately after irradiation, 100 μL of the mixture in each well, containing 1 × 10⁴ CFU of each microorganism, was transferred to an agar plate (ø 100 mm) containing agar powder in an appropriate liquid medium. *Staphylococcus aureus* and *P. aeruginosa* were incubated for 24 to 36 h at 37 °C, and *C. albicans* was incubated for 72 to 84 h at 24 °C for colony enumeration. If the number of colonies formed was under 300 CFU per plate, it was regarded as detectable.

3. Results

3.1. Absorption Spectra of the Photosensitizers

The absorption spectra of TONS504 dissolved in both PBS and PBS/TX100 showed a Soret band at around 400–420 nm and a Q band at around 665 nm at all concentrations (Fig. 2). In short, TONS504 had a widespread absorption range between 300 nm to 700 nm with several peaks. The Soret band of TONS504 was divided into two peaks at around 400 nm and 420 nm. The 420 nm peak became smaller than the 400 nm peak as the concentration of TONS504 increased. This shift, with the absorption maximum shifting to a shorter wavelength when a dye self-aggregates (Fig. 2a), is called metachromasy [31]. By contrast, when TONS504 was dissolved in PBS/TX100, the highest peak occurred at around 420 nm, and the ratio of the peaks at around 400 nm and 420 nm did not change with changes in the concentration (Fig. 2b). These results suggested that TONS504 aggregation in PBS caused the change in the ratio between the two peaks at 400 and 420 nm, and that TONS504 did not aggregate in PBS/TX100. The absorption spectra of MB under all conditions similarly exhibited a single peak at around 663 nm (Fig. 3). The amplitude of the peak changed in proportion to the MB concentration both in PBS and PBS/TX100; however, the peak did not shift with changes in the conditions. These results suggested that MB dissolved well in both PBS and PBS/TX100 regardless of its concentration.

3.2. Detection of the ¹O₂ Luminescence

Fig. 4a shows ¹O₂ luminescence decay curves of 1 μmol/L TONS504 and MB dissolved in PBS, and Fig. 4b shows decay curves of the photosensitizers in PBS/TX100. The initial spike emerging before 80 ns was ignorable noise originating from fluorescence and scattering. The decay curve was integrated after background removal to obtain the area intensity. Table 1 lists the area intensity for each condition obtained from the integrated value. The area intensity ratio is equal to the ratio of the ¹O₂ quantum yield. The area intensities of TONS504 in PBS and PBS/TX100 were about 0.9-fold lower and about 2.1-fold higher than the average area intensity of MB, respectively.

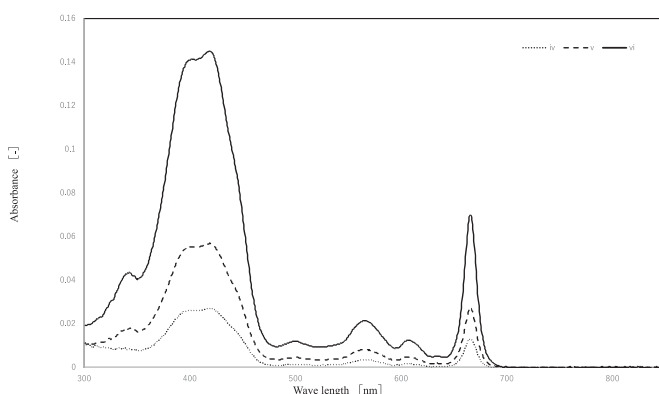
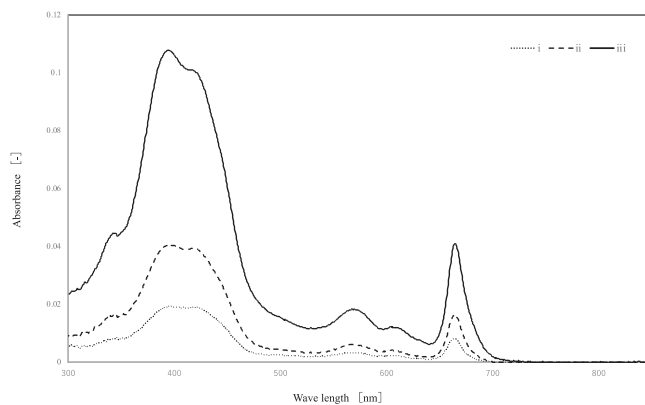


Fig. 2. a Absorption spectra of TONS504 dissolved in PBS at (i) 1 μmol/L, (ii) 2 μmol/L, and (iii) 5 μmol/L.

b Absorption spectra of TONS504 dissolved in PBS/TX100 at (iv) 1 μmol/L, (v) 2 μmol/L, and (vi) 5 μmol/L.

b Time-resolved luminescence of ¹O₂ generated by 1 μmol/L (iii) MB and (iv) TONS504 in PBS/TX100.

3.3. PAEs and Dark Toxicity with *S. aureus*

With light irradiation, TONS504 and MB showed apparent antimicrobial effects on *S. aureus* (Table 2). PACT with 9.0 × 10⁻² μmol/L TONS504 decreased the bacteria to the detectable range but some of the colonies remained (108.2 ± 70.9 CFU). TONS504 at 9.0 × 10⁻² to 9.0 μmol/L and MB at 9.0–900 μmol/L eliminated the bacteria completely, which corresponded to a reduction of more than 4 log₁₀ CFU. Light irradiation without the photosensitizers did not show any toxicity toward the bacteria. In the absence of light irradiation, 9.0 μmol/L TONS504 eliminated the bacteria. By contrast, the number of colonies of bacteria was not reduced to the detectable range by MB without light irradiation.

3.4. PAEs and Dark Toxicity with *P. aeruginosa*

PACT with TONS504 and MB also showed an antimicrobial effect toward *P. aeruginosa* (Table 3). PACT with 9.0 μmol/L TONS504 and 9.0–900 μmol/L MB completely eliminated the bacteria. Controls with light irradiation alone or the photosensitizers alone did not show cytotoxicity toward *P. aeruginosa*.

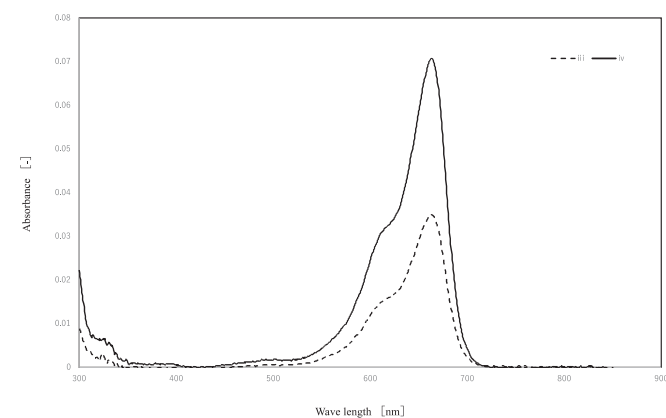
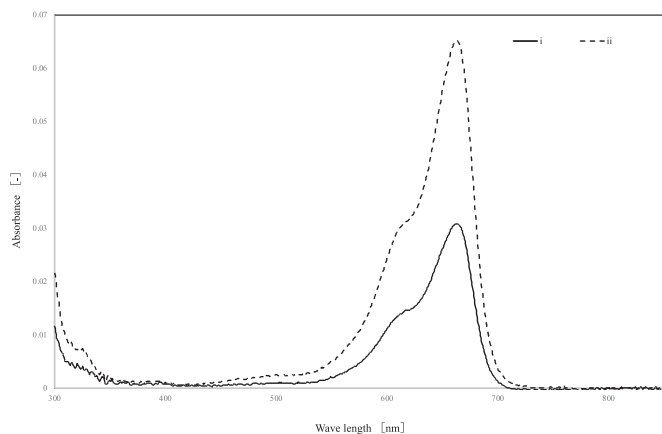


Fig. 3. **a** Absorption spectra of MB dissolved in PBS at (i) 1 $\mu\text{mol/L}$ and (ii) $\mu\text{mol/L}$. **b** Absorption spectra of MB dissolved in PBS/TX100 at (iii) 1 $\mu\text{mol/L}$ and (iv) 2 $\mu\text{mol/L}$.

3.5. PAEs and Dark Toxicity with *C. albicans*

The viability of *C. albicans* decreased with PACT with both TONS504 and MB (Table 4). TONS504 at 9.0 $\mu\text{mol/L}$ inactivated *C. albicans* completely. MB at 90 $\mu\text{mol/L}$ reduced the viability of the fungi to the detectable range, but MB did not completely eliminate the fungi at any concentration. MB at the highest concentration (900 $\mu\text{mol/L}$) did not reduce *C. albicans* to the detectable range. Controls with light irradiation alone or the photosensitizers alone did not show cytotoxicity toward *C. albicans*.

4. Discussion

We found that TONS504 exhibited higher $^1\text{O}_2$ quantum yields than MB in PBS/TX100 but not in PBS. In addition, TONS504 showed apparent PAEs on *S. aureus* and *C. albicans* at a lower concentration than MB. By contrast, the apparent PAEs for TONS504 and MB on *P. aeruginosa* occurred at the same concentration.

The difference in the $^1\text{O}_2$ quantum yields with TONS504 between PBS and PBS/TX100 can be explained by aggregation of TONS504 in the solutions. The absorption spectra suggested that TONS504 aggregated when dissolved in PBS, but not in PBS/TX100. Self-aggregation of photosensitizers limits the efficiency of $^1\text{O}_2$ generation [32]. TONS504 consists of a hydrophobic chlorin ring and hydrophilic side-chains containing one hydroxy group and pyridinium groups (Fig. 1). The side-chains make TONS504 water-soluble, but TONS504 still tends to

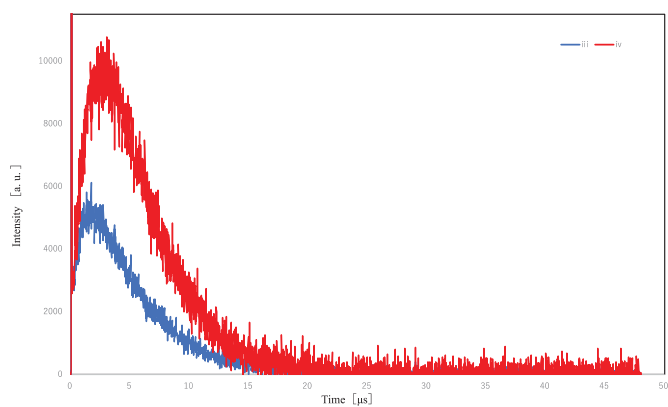
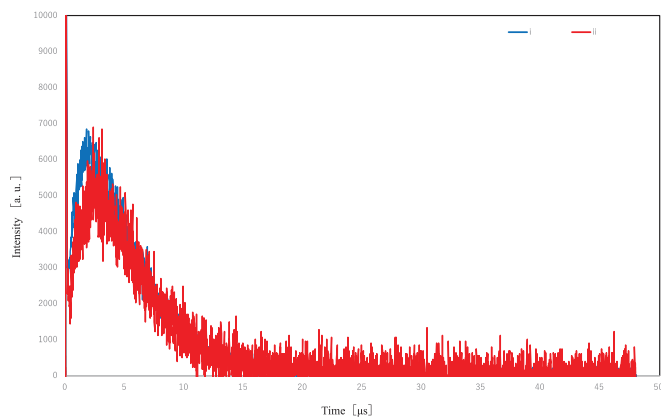


Fig. 4. **a** Time-resolved luminescence of $^1\text{O}_2$ generated by 1 $\mu\text{mol/L}$ (i) MB and (ii) TONS504 in PBS.

Table 1

The area intensity of $^1\text{O}_2$ luminescence generated from TONS504 and methylene blue.

	solvent	Concentration of photosensitizers ($\mu\text{mol/L}$)		
		1	2	5
MB	PBS	0.042	0.0421	
	PBS/TX100	0.0343	0.0351	
TONS504	PBS	0.0369	0.0392	0.0374
	PBS/TX100	0.0717	0.0721	0.0755

self-aggregate in water or PBS because of the hydrophobic chlorin ring. As a surfactant, TX100 inhibits TONS504 self-aggregation, and hence the $^1\text{O}_2$ quantum yield of TONS504 is about 2.1-fold higher than that of MB in PBS/TX100 in the monomer form. We speculated that the cell walls of the microorganisms might inhibit TONS504 self-aggregation because of their surface hydrophobicity [33–35]. This corresponds with our results that TONS504 exhibited PAEs on various microorganisms that were equal to or greater than those of MB. However, by contrast, Usacheva et al. reported that the presence of bacteria promoted self-aggregation of MB and toluidine blue [36]. It is difficult to determine whether microorganisms accelerate or inhibit the self-aggregation of photosensitizers, because the answer likely depends on the concentrations of the microorganisms and photosensitizers. Therefore, it is challenging to determine which photosensitizer generates $^1\text{O}_2$ more efficiently in the presence of microorganisms.

In the latter part of this study, we evaluated the antimicrobial effects

Table 2
Photodynamic antimicrobial effects of TONS504 and methylene blue (MB) on *S. aureus*.

	Light irradiation	Concentrations of the photosensitizers ($\mu\text{mol/L}$)						
		0	9.0×10^{-3}	9.0×10^{-2}	9.0×10^{-1}	9.0	90	900
TONS504	+	>300	>300	108.2 ± 70.9	0	0		
	-	>300	>300	>300	>300	0		
MB	+	>300			>300	0	0	0
	-	>300			>300	>300	>300	>300

Data represents colony numbers per agar plate. + indicates photosensitizer exposure with light irradiation. - indicates photosensitizer exposure alone.

Table 3
Photodynamic antimicrobial effects of TONS504 and methylene blue (MB) on *P. aeruginosa*.

	Light irradiation	Concentrations of the photosensitizers ($\mu\text{mol/L}$)						
		0	9.0×10^{-3}	9.0×10^{-2}	9.0×10^{-1}	9.0	90	900
TONS504	+	>300	>300	>300	>300	0		
	-	>300	>300	>300	>300	>300		
MB	+	>300			>300	0	0	0
	-	>300			>300	>300	>300	>300

Data represents colony numbers per agar plate. + indicates photosensitizer exposure with light irradiation. - indicates photosensitizer exposure alone.

Table 4
Photodynamic antimicrobial effects of TONS504 and methylene blue (MB) on *C. albicans*.

	Light irradiation	Concentrations of the photosensitizers ($\mu\text{mol/L}$)						
		0	9.0×10^{-3}	9.0×10^{-2}	9.0×10^{-1}	9.0	90	900
TONS504	+	>300	>300	>300	>300	0		
	-	>300	>300	>300	>300	>300		
MB	+	>300			>300	>300	119.2 ± 20.0	>300
	-	>300			>300	>300	>300	>300

Data represents colony numbers per agar plate. + indicates photosensitizer exposure with light irradiation. - indicates photosensitizer exposure alone.

of TONS504 and MB. Neither MB alone nor light irradiation alone inhibited the growth of any bacteria, but TONS504 at $9.0 \mu\text{mol/L}$, the highest concentration, exhibited dark toxicity toward *S. aureus*. By contrast, Latief et al. reported that TONS504 at the same concentration did not show dark toxicity toward *S. aureus* [23]. The only difference between the two experiments was the solvent used to prepare the TONS504 solution. Latief et al. dissolved TONS504 in Mueller Hinton broth, whereas we used PBS as the solvent in the present study. Several studies have investigated the dark toxicity of photosensitizers, such as rose bengal, erythrosine, toluidine blue, and MB [36–38]. They concluded that those photosensitizers acted as bactericides at high concentrations in PBS or 0.45% saline. Although the protective mechanism of Muller Hinton broth for the bacteria is unclear, it seems certain that some photosensitizers such as TONS504 have cytotoxicity at high concentrations even without light irradiation.

With light irradiation, the minimum molar concentration of TONS504 ($9.0 \times 10^{-2} \mu\text{mol/L}$) that reduced *S. aureus* to the detectable range was one-hundredth that of MB ($9.0 \mu\text{mol/L}$). When comparing the concentration needed to achieve complete colony elimination, corresponding to a reduction of over $4 \log_{10}$ CFU, the concentration of TONS504 was one-tenth that of MB. By contrast, *P. aeruginosa* elimination was achieved with the same concentration of TONS504 and MB ($9.0 \mu\text{mol/L}$). This concentration was also the same as that required for light-activated MB elimination of *S. aureus*. As stated above, TONS504 generates more $^1\text{O}_2$ than MB, and $^1\text{O}_2$ is one of the critical factors affecting the efficacy of photodynamic therapy [39]. The difference in $^1\text{O}_2$ generation may partially explain why TONS504 exhibited PAE on *S. aureus* at lower concentrations than MB. However, the hypothesis that the $^1\text{O}_2$ quantum yield is the exclusive or dominant factor of PAE cannot explain why the growth of *P. aeruginosa* was inhibited by TONS504 and MB at the same concentration. This paradox is in line with a previous study that found MB generated more $^1\text{O}_2$ than toluidine blue ortho but

toluidine blue ortho was more effective than MB at removing *Streptococcus mutans* [37]. Except for the $^1\text{O}_2$ quantum yields, other differences between TONS504 and MB that could potentially affect the PAE are their molecular weights and partition coefficients [40,41]. Whereas Gram-positive bacteria possess a permeable cell wall composed of peptidoglycan and anionic polymers, which allows molecules with molecular weights in the range 30,000–57,000 Da to penetrate [42], Gram-negative bacteria possess an outer membrane composed of lipopolysaccharide (LPS) and other lipoproteins sandwiching the peptidoglycan layer [43,44]. The outer membrane of Gram-negative bacteria strongly inhibits the penetration of molecules and plays an important role in their resistance to antibiotics and photosensitizers [44]. However, there are several pathways through which molecules can penetrate the outer membrane. The first pathway, called the self-promoted uptake pathway, relates to LPS [45]. LPS is negatively charged and binds divalent cations strongly [43]. The association between LPS and divalent cations contributes to the integrity of the outer membrane of Gram-negative bacteria [43]. Cationic molecules disrupt the association between LPS and divalent cations and consequently break through the outer membrane, regardless of their molecular weight [41,43]. Both TONS504 and MB are cationic photosensitizers and taken up by the self-promoted uptake pathway, and hence both exhibit PAEs on *P. aeruginosa*. Another pathway to penetrate the outer membrane is through aqueous channels of proteins called porins [43]. Porins allow “only relatively hydrophilic compounds with a molecular weight lower than 600–700 Da” to pass into the cellular membrane [41]. The molecular weight of TONS504 is too high for it to pass through porins, while the molecular weight of MB is low enough. We assumed that MB passing through porins neutralized the disadvantage of the $^1\text{O}_2$ quantum yield against TONS504. The other difference between TONS504 and MB is their partition coefficients. We calculated the partition coefficients of TONS504 and MB using Chem-Draw and found that the log *P* of the partition coefficient of TONS504

was 7.2688 less than that of MB (0.9495). Photosensitizers with higher partition coefficients accumulate in the hydrophobic region of the cellular membrane and may damage the target bacteria. Rolim et al. also speculated that the partition coefficient likely affected the PAE difference between MB and toluidine blue [37].

The present study is the first to show that TONS504-PACT is effective on *C. albicans*. TONS504 reduced *C. albicans* to the detectable range at a lower concentration than MB. Moreover, TONS504 completely eliminated the fungal colonies, whereas MB did not. The minimum molar density of TONS504 exhibited an apparent antimicrobial effect on *C. albicans* that was same as that on *P. aeruginosa* and 100-fold higher than that on *S. aureus*. For MB, the minimum molar density on *C. albicans* was 100-fold higher than those on *S. aureus* and *P. aeruginosa*. The external walls of fungi are more permeable than the outer membranes of Gram-negative bacteria, and hence fungi should be more sensitive to PACT than Gram-negative bacteria [42]. One possible reason why *C. albicans* showed such a strong resistance to PACT in the present study is the multidrug efflux systems (MESs) of fungi. MESs, belonging to the ATP-binding cassette (ABC) or the major facilitator superfamily, are the mechanisms through which fungi acquire resistance to azole antifungals [45]. Prates et al. reported that an ABC MES inhibited the uptake of MB by *C. albicans* and the MB PAE [45]. Although it is still unclear if an ABC MES also inhibits TONS504-PACT, MESs likely contributed to the PACT-resistance of *C. albicans* in the present study.

Interestingly, PACT reduced *C. albicans* to the detectable range with 90 $\mu\text{mol/L}$ MB but not with 900 $\mu\text{mol/L}$ MB. Da Collina et al. reported that MB exhibited the strongest PAE at 10 $\mu\text{g/mL}$, corresponding to 33.3 $\mu\text{mol/L}$, and the effect decreased at higher concentrations [46]. They stated in their discussion that self-aggregation of MB likely occurred at high concentrations and decreased the PAE [46]. To the best of our knowledge, the PAE of TONS504 increases in a concentration dependent manner [21–26]; however, the PAE of TONS504 may also decrease at higher concentrations than we have tested, given its strong tendency to self-aggregate.

This study has a potential limitation. In the latter part, we set the concentration of every microbial suspension to 1×10^7 CFU/mL and evaluated the minimum molar density of photosensitizer required to reduce the microorganisms to the detectable range. We tested no other microbial suspension concentration, so the PAE was not quantified. However, the PAE was basically concentration dependent except at very high concentrations.

Further studies, such as identification of adjunctive drugs to boost TONS 504-PACT or evaluation of the efficacy in animal models, are required. It is important to emphasize that this study is the first to report the molecular characteristics of TONS504. We believe the present study provides a basis for further in vitro and in vivo studies.

Funding

This work was supported by the Japan Society for the Promotion of Science (JSPS) Kakenhi Grants-in-Aid for Scientific Research (C) [grant numbers 15K10894 and 18K09411]; and the Tsuchiya Memorial Foundation [grant number 2017–2018].

Authorship statement

None.

Declaration of Competing Interest

None.

Acknowledgements

We thank Isao Sakata (Porphyrin Laboratory, Okayama, Japan) for providing information on TONS504 and Akira Ichikawa (CCS, Kyoto,

Japan) for constructing the LED device according to our design.

References

- [1] S.R. Flaxman, R.R.A. Bourne, S. Resniko, P. Ackland, T. Braithwaite, M. V Cicinelli, A. Das, J.B. Jonas, J. Kee, J.H. Kempen, J. Leasher, H. Limburg, K. Naidoo, K. Pesudovs, A. Silvester, G.A. Stevens, N. Tahhan, T.Y. Wong, Global causes of blindness and distance vision impairment 1990–2020 : A systematic review and meta-analysis, *lancet glob. Heal.* 5 (2020) 1221–1234. doi:[https://doi.org/10.1016/S2214-109X\(17\)30393-5](https://doi.org/10.1016/S2214-109X(17)30393-5).
- [2] L. Ung, P.J.M. Bispo, S.S. Shanbhag, M.S. Gilmore, J. Chodosh, The persistent dilemma of microbial keratitis: global burden, diagnosis, and antimicrobial resistance, *Surv. Ophthalmol.* 64 (2019) 255–271. <https://doi.org/10.1016/j.survophthal.2018.12.003>.
- [3] K.J. Ray, L. Prajna, M. Srinivasan, M. Geetha, R. Karpagam, D. Glidden, C. E. Oldenburg, C.Q. Sun, S.D. McLeod, N.R. Acharya, T.M. Lietman, Fluoroquinolone treatment and susceptibility of isolates from bacterial keratitis, *JAMA Ophthalmol.* 131 (2013) 310–313. <https://doi.org/10.1001/jamaophthalmol.2013.1718>.
- [4] N. Venkatesh Prajna, P. Lalitha, R. Rajaraman, T. Krishnan, A. Raghavan, M. Srinivasan, K.S. O'Brien, M. Zegans, S.D. McLeod, N.R. Acharya, J.D. Keenan, T. M. Lietman, J. Rose-Nussbaumer, J. Mascarenhas, R. Karpagam, M. Rajkumar, S. R. Sumithra, C. Sundar, P. Manikandan, N. Shivananda, J.P. Whitcher, S. Lee, B. L. Shapiro, C.E. Oldenburg, K.C. Hong, M. Fisher, A. Aldave, D. Everett, J. Glover, K. Ananda Kannan, S. Kymes, I. Schwab, D. Glidden, K. Ray, V. Cevallos, C.M. Kidd, Changing azole resistance: A secondary analysis of the MUTT I randomized clinical trial, *JAMA Ophthalmol.* 134 (2016) 693–696. <https://doi.org/10.1001/jamaophthalmol.2016.0530>.
- [5] F. Cieplika, D. Dengb, W. Crielaard, W. Buchalla, E. Hellwig, A. Al-Ahmad, T. Misch, Antimicrobial photodynamic therapy - what we know and what we don't, *Crit. Rev. Microbiol.* 44 (2018) 571–589. <https://doi.org/10.1080/1040841X.2018.1467876>.
- [6] M. Wainwright, Photodynamic antimicrobial chemotherapy (PACT), *J. Antimicrob. Chemother.* 42 (1998) 13–28. <https://doi.org/10.1093/jac/42.1.13>.
- [7] F. Vatanserver, W.C.M.A. de Melo, P. Avci, D. Vecchio, M. Sadasivam, A. Gupta, R. Chandran, M. Karimi, N.A. Parizzotto, R. Yin, G.P. Tegos, M.R. Hamblin, Antimicrobial strategies centered around reactive oxygen species - bactericidal antibiotics, photodynamic therapy, and beyond, *FEMS Microbiol. Rev.* 37 (2013) 955–989. <https://doi.org/10.1111/1574-6976.12026>.
- [8] M. Wainwright, T. Maisch, S. Nonell, K. Plaetzer, A. Almeida, G.P. Tegos, M. R. Hamblin, Photoantimicrobials—are we afraid of the light? *Lancet Infect. Dis.* 17 (2017) e49–e55. [https://doi.org/10.1016/S1473-3099\(16\)30268-7](https://doi.org/10.1016/S1473-3099(16)30268-7).
- [9] S.A.R. Martins, J.C. Combs, G. Noguera, W. Camacho, P. Wittmann, R. Walther, M. Cano, J. Dick, A. Behrens, Antimicrobial efficacy of riboflavin/UVA combination (365 nm) in vitro for bacterial and fungal isolates: a potential new treatment for infectious keratitis, *Investig. Ophthalmol. Vis. Sci.* 49 (2008) 3402–3408. <https://doi.org/10.1167/iovs.07-1592>.
- [10] D.G. Said, M.S. Elalfy, Z. Gatzoufas, E.S. El-Zakouk, M.A. Hassan, M.Y. Saif, A. A. Zaki, H.S. Dua, F. Hafezi, Collagen cross-linking with photoactivated riboflavin (PACK-CXL) for the treatment of advanced infectious keratitis with corneal melting, *Ophthalmology.* 121 (2014) 1377–1382. <https://doi.org/10.1016/j.ophtha.2014.01.011>.
- [11] D. Tabibian, C. Mazzotta, F. Hafezi, PACK-CXL: corneal cross-linking in infectious keratitis, *Eye Vis.* 3 (2016) 1–5. <https://doi.org/10.1186/s40662-016-0042-x>.
- [12] X. Qin, X. Sun, J. Lu, PACK-CXL: corneal collagen cross-linking for infectious keratitis, *Zhonghua Shiyang Yanke Zazhi/Chinese J. Exp. Ophthalmol.* 36 (2018) 570–575. <https://doi.org/10.3760/cma.j.issn.2095-0160.2018.07.018>.
- [13] M.S. Norm, Vital staining of the cornea and conjunctiva with a mixture of fluorescein and rose Bengal, *Am J. Ophthalmol.* 64 (1967) 1078–1080. [https://doi.org/10.1016/0002-9394\(67\)93058-9](https://doi.org/10.1016/0002-9394(67)93058-9).
- [14] A. Arboleda, D. Miller, F. Cabot, M. Taneja, M.C. Aguilar, K. Alawa, G. Amescua, S. H. Yoo, J.M. Parel, Assessment of rose bengal versus riboflavin photodynamic therapy for inhibition of fungal keratitis isolates, *Am J. Ophthalmol.* 158 (2014). <https://doi.org/10.1016/j.ajo.2014.04.007>.
- [15] F. Halili, A. Arboleda, H. Durkee, M. Taneja, D. Miller, K.A. Alawa, M.C. Aguilar, G. Amescua, H.W. Flynn, J.M. Parel, Rose Bengal- and riboflavin-mediated photodynamic therapy to inhibit methicillin-resistant *Staphylococcus aureus* keratitis isolates, *Am J. Ophthalmol.* 166 (2016) 194–202. <https://doi.org/10.1016/j.ajo.2016.03.014>.
- [16] A. Naranjo, A. Arboleda, J.D. Martinez, H. Durkee, M.C. Aguilar, N. Relhan, N. Nikpoor, A. Galor, S.R. Dubovy, H.W. Flynn, D. Miller, J.M. Parel, G. Amescua, R. Leblanc, Rose Bengal photodynamic antimicrobial therapy for patients with progressive infectious keratitis: a pilot clinical study, *Am J. Ophthalmol.* 214 (2020) 198–200. <https://doi.org/10.1016/j.ajo.2020.02.001>.
- [17] G.B. Kharkwal, S.K. Sharma, Y.Y. Huang, T. Dai, M.R. Hamblin, Photodynamic therapy for infections: clinical applications, *Lasers Surg. Med.* 43 (2011) 755–767. <https://doi.org/10.1002/lsm.21080>.
- [18] C. Spagnol, L.C. Turner, R.W. Boyle, Journal of photochemistry and photobiology B : biology immobilized photosensitizers for antimicrobial applications, *J. Photochem. Photobiol. B Biol.* 150 (2015) 11–30. <https://doi.org/10.1016/j.jphotobiol.2015.04.021>.
- [19] A. Felgentrager, T. Maisch, D. Dobler, A. Spath, Hydrogen bond acceptors and additional cationic charges in methylene blue derivatives: photophysics and antimicrobial efficiency, *BioMed Reserch Int.* (2013). <https://doi.org/10.1155/2013/482167>.

- [20] L. Bourré, F. Giuntini, I.M. Eggleston, C.A. Mosse, A.J. MacRobert, M. Wilson, Effective photoinactivation of gram-positive and gram-negative bacterial strains using an HIV-1 tat peptide-porphyrin conjugate, *Photochem. Photobiol. Sci.* 9 (2010) 1613–1620, <https://doi.org/10.1039/c0pp00146e>.
- [21] K. Sueoka, T. Chikama, Y.D. Pertiwi, J.A. Ko, Y. Kiuchi, T. Sakaguchi, A. Obana, Antifungal efficacy of photodynamic therapy with TONS 504 for pathogenic filamentous fungi, *Lasers Med. Sci.* 34 (2019) 743–747, <https://doi.org/10.1007/s10103-018-2654-y>.
- [22] Y.D. Pertiwi, T. Chikama, K. Sueoka, J.A. Ko, Y. Kiuchi, M. Onodera, T. Sakaguchi, Photodynamic antimicrobial chemotherapy with the photosensitizer TONS504 eradicates *Acanthamoeba*, *Photodiagn. Photodyn. Ther.* 28 (2019) 166–171, <https://doi.org/10.1016/j.pdpdt.2019.08.035>.
- [23] M.A. Latief, T. Chikama, M. Shibasaki, T. Sasaki, J.A. Ko, Y. Kiuchi, T. Sakaguchi, A. Obana, Antimicrobial action from a novel porphyrin derivative in photodynamic antimicrobial chemotherapy in vitro, *Lasers Med. Sci.* 30 (2014) 383–387, <https://doi.org/10.1007/s10103-014-1681-6>.
- [24] M.A. Latief, T. Chikama, J.A. Ko, Y. Kiuchi, T. Sakaguchi, A. Obana, Inactivation of acyclovir-sensitive and -resistant strains of herpes simplex virus type 1 in vitro by photodynamic antimicrobial chemotherapy, *Mol. Vis.* 21 (2015) 532–537.
- [25] K. Sueoka, T. Chikama, M.A. Latief, J.A. Ko, Y. Kiuchi, T. Sakaguchi, A. Obana, Time-dependent antimicrobial effect of photodynamic therapy with TONS 504 on *Pseudomonas aeruginosa*, *Lasers Med. Sci.* 33 (2018) 1455–1460, <https://doi.org/10.1007/s10103-018-2490-0>.
- [26] Y.D. Pertiwi, T. Chikama, K. Sueoka, J.A. Ko, Y. Kiuchi, M. Onodera, T. Sakaguchi, Efficacy of photodynamic anti-microbial chemotherapy for *Acanthamoeba keratitis* in vivo, *Lasers Surg. Med.* (2020), <https://doi.org/10.1002/lsm.23355> in press.
- [27] M. Wilson, Photolysis of oral bacteria and its potential use in the treatment of caries and periodontal disease, *J. Appl. Bacteriol.* 75 (1993) 299–306, <https://doi.org/10.1111/j.1365-2672.1993.tb02780.x>.
- [28] R. Boltes Cecatto, L. Siqueira de Magalhães, M. Fernanda Setúbal Destro Rodrigues, C. Pavani, A. Lino-dos-Santos-Franco, M. Teixeira Gomes, D. Fátima Teixeira Silva, Methylene blue mediated antimicrobial photodynamic therapy in clinical human studies: The state of the art, *Photodiagn. Photodyn. Ther.* 31 (2020), <https://doi.org/10.1016/j.pdpdt.2020.101828>.
- [29] S. Okazaki, T. Tomo, M. Mimuro, Direct measurement of singlet oxygen produced by four chlorin-ringed chlorophyll species in acetone solution, *Chem. Phys. Lett.* 485 (2010) 202–206, <https://doi.org/10.1016/j.cplett.2009.12.055>.
- [30] T. Nishimura, K. Hara, N. Honda, S. Okazaki, H. Hazama, K. Awazu, Determination and analysis of singlet oxygen quantum yields of talaporfin sodium, protoporphyrin IX, and lipidated protoporphyrin IX using near-infrared luminescence spectroscopy, *Lasers Med. Sci.* 35 (2020) 1289–1297, <https://doi.org/10.1007/s10103-019-02907-0>.
- [31] M.N. Usacheva, M.C. Teichert, M.A. Biel, The role of the methylene blue and toluidine blue monomers and dimers in the photoinactivation of bacteria, *J. Photochem. Photobiol. B Biol.* 71 (2003) 87–98, <https://doi.org/10.1016/j.jphotobiol.2003.06.002>.
- [32] A.F. Uchoa, K.T. De Oliveira, M.S. Baptista, A.J. Bortoluzzi, Y. Yamamoto, O. A. Serra, Chlorin photosensitizers sterically designed to prevent self-aggregation, *J. Organomet. Chem.* 76 (2011) 8824–8832, <https://doi.org/10.1021/jo201568n>.
- [33] F. Reifsteck, S. Wee, B.J. Wllknsont, Hydrophobicity-hydrop hilicity of staphylococci, *J. Med. Microbiol.* 24 (1987) 65–73, <https://doi.org/10.1099/00222615-24-1-65>.
- [34] E. Vanhaecke, J.P. Remon, M. Moors, F. Raes, D. De Rudder, A. Van Peteghem, Kinetics of *Pseudomonas aeruginosa* adhesion to 304 and 316-L stainless steel: role of cell surface hydrophobicity, *Appl. Environ. Microbiol.* 56 (1990) 788–795, <https://doi.org/10.1128/aem.56.3.788-795.1990>.
- [35] R.R. Goswami, S.D. Pohare, J.S. Raut, S. Mohan Karuppappil, Cell surface hydrophobicity as a virulence factor in *Candida albicans*, *Biosci. Biotechnol. Res. Asia* 14 (2017) 1503–1511, <https://doi.org/10.13005/bbra/2598>.
- [36] M.N. Usacheva, M.C. Teichert, M.A. Biel, The role of the methylene blue and toluidine blue monomers and dimers in the photoinactivation of bacteria, *J. Photochem. Photobiol. B Biol.* 71 (2003) 87–98, <https://doi.org/10.1016/j.jphotobiol.2003.06.002>.
- [37] J.P.M.L. Rolim, M.A.S. De-Melo, S.F. Guedes, F.B. Albuquerque-Filho, J.R. De Souza, N.A.P. Nogueira, I.C.J. Zanin, L.K.A. Rodrigues, The antimicrobial activity of photodynamic therapy against *Streptococcus mutans* using different photosensitizers, *J. Photochem. Photobiol. B Biol.* 106 (2012) 40–46, <https://doi.org/10.1016/j.jphotobiol.2011.10.001>.
- [38] T.P. Paulino, K.F. Ribeiro, G. Thedei, A.C. Tedesco, P. Ciancaglini, Use of hand held photopolymerizer to photoinactivate *Streptococcus mutans*, *Arch. Oral Biol.* 50 (2005) 353–359, <https://doi.org/10.1016/j.archoralbio.2004.09.002>.
- [39] E.S. Nyman, P.H. Hynninen, Research advances in the use of tetrapyrrolic photosensitizers for photodynamic therapy, *J. Photochem. Photobiol. B Biol.* 73 (2004) 1–28, <https://doi.org/10.1016/j.jphotobiol.2003.10.002>.
- [40] S.J. Wagner, A. Skripchenko, D. Robinette, J.W. Foley, L. Cincotta, Factors affecting virus Photoinactivation by a series of phenothiazine dyes, *Photochem. Photobiol.* 67 (1998) 343–349, <https://doi.org/10.1111/j.1751-1097.1998.tb05208.x>.
- [41] G. Jori, C. Fabris, M. Soncin, S. Ferro, O. Coppellotti, D. Dei, L. Fantetti, G. Chiti, G. Roncucci, Photodynamic therapy in the treatment of microbial infections: basic principles and perspective applications, *Lasers Surg. Med.* 38 (2006) 468–481, <https://doi.org/10.1002/lsm.20361>.
- [42] P.A. Lambert, Cellular impermeability and uptake of biocides and antibiotics in gram-positive bacteria and mycobacteria, *J. Appl. Microbiol. Symp. Suppl.* 92 (2002) 46–54, <https://doi.org/10.1046/j.1365-2672.92.5s1.7.x>.
- [43] R.E.W. Hancock, A. Bell, Antibiotic uptake into gram-negative bacteria, *Curr. Top. Infect. Dis. Clin. Microbiol.* 2 (1989) 21–28, https://doi.org/10.1007/978-3-322-86064-4_5.
- [44] F.F. Sperandio, Y.Y. Huang, M.R. Hamblin, Antimicrobial photodynamic therapy to kill gram-negative Bacteria, *Recent Pat. Antiinfect. Drug Discov.* 8 (2013) 108–120, <https://doi.org/10.2174/1574891x113089990012>.
- [45] R.A. Prates, I.T. Kato, M.S. Ribeiro, G.P. Tegos, M.R. Hamblin, Influence of multidrug efflux systems on methylene blue-mediated photodynamic inactivation of *Candida albicans*, *J. Antimicrob. Chemother.* 66 (2011) 1525–1532, <https://doi.org/10.1093/jac/dkr160>.
- [46] G.A. Da Collina, F. Freire, T.P. Da C. Santos, N.G. Sobrinho, S. Aquino, R.A. Prates, D. De F.T. Da Silva, A.C.R. Tempestini Horliana, C. Pavani, Controlling methylene blue aggregation: a more efficient alternative to treat *Candida albicans* infections using photodynamic therapy, *Photochem. Photobiol. Sci.* 17 (2018) 1355–1364, <https://doi.org/10.1039/C8PP00238J>.